Nonlinear Pavement Foundation Modeling for Three-Dimensional Finite-Element Analysis of Flexible Pavements

Minkwan Kim, A.M.ASCE[1]; Erol Tutumluer, M.ASCE[2]; and Jayhyun Kwon[3]

Abstract: Pavement foundation geomaterials, i.e., fine-grained subgrade soils and unbound aggregates used in untreated base/subbase layers, exhibit nonlinear behavior under repeated wheel loads. This nonlinear behavior is commonly characterized by stress-dependent resilient modulus material models that need to be incorporated into finite element (FE) based mechanistic pavement analysis methods to predict more accurately the pavement resilient responses, such as stress, strain, and deformation. Many general-purpose FE programs have been used to predict such pavement responses under various traffic loading conditions while not considering properly material characterizations of the unbound aggregate base/subbase and subgrade soil layers. This paper describes the recent pavement FE modeling research efforts at the University of Illinois focused on using both the specific-purpose axisymmetric and general-purpose three-dimensional (3D) FE programs for flexible pavement analyses. To properly characterize the resilient behavior of pavement foundations, nonlinear stress-dependent modulus models have been programmed in a *user material subroutine* (UMAT) in the commercial general-purpose finite-element program ABAQUS. The results indicated that proper characterizations of the nonlinear stress-dependent geomaterials significantly impacted accurate predictions of critical pavement responses. The prediction ability of the developed nonlinear UMAT characterization was next validated by predicting similar pavement critical responses to those measured from field instrumented pavement test sections. Different resilient modulus models, considering both axisymmetric and 3D stress states, developed from true triaxial test data on unbound granular materials were also studied. When the intermediate principal stresses were taken into account in the 3D modulus model development unlike in the axisymmetric models, somewhat lower asphalt concrete tensile strains were obtained from 3D nonlinear FE analyses of flexible pavements with unbound aggregate bases.

DOI: 10.1061/(ASCE)1532-3641(2009)9:5(195)

CE Database subject headings: Nonlinear analysis; Stress; Aggregates; Subgrades; Finite element method; Flexible pavements.

Introduction

Flexible pavements are most commonly used for low to medium volume roads with significant usage also found in high volume interstate highways and airfield runways, taxiways and aprons subjected to heavy aircraft gear/wheel loads. As the demand for applied wheel loads and number of load applications increases, it becomes very important to properly characterize the behavior of subgrade soils and unbound aggregate layers as the foundations of the layered pavement structure. Unfortunately, most commonly used elastic layered programs assume linear elastic material behavior for the unbound aggregate base/subbase and subgrade soil layers. Previous laboratory studies have shown that the resilient responses of both coarse-grained unbound granular materials used in untreated base/subbase courses and fine-grained subgrade follow nonlinear, stress-dependent behavior under repeated traffic loading (Brown and Pappin 1981; Uzan 1985; Thompson and Elliott 1985; Tutumluer 1995; Rowshanzamir 1995). Unbound granular materials exhibit stress hardening, whereas, fine-grained soils show stress-softening type behavior. A finite element (FE) type analysis needs to be employed to model such nonlinear resilient behavior and more realistically predict pavement responses for a mechanistic pavement analysis.

FE based structural analysis has been the main mechanistic approach for analyzing flexible pavements due to its ability to incorporate advanced material characterization models to predict more accurately the wheel load induced responses, such as deformations, stresses, and strains in the pavement structure. Several well known axisymmetric pavement FE analysis models, such as the validated ILLI-PAVE and GT-PAVE programs, properly considered nonlinear pavement foundation geomaterial behavior (Raad and Figueroa 1980; Tutumluer 1995). Numerous attempts using general-purpose FE programs, such as ABAQUS, ANSYS, and ADINA, have also been made to predict pavement responses under various pavement geometry and loading conditions (Hjelmstad and Taciroglu 2000; Schwartz 2002; Sukumaran et al. 2004; Saad et al. 2005). With ongoing advances in computer technology and numerical solution techniques, general-purpose FE programs can now especially deal with larger and more computationally intense three-dimensional (3D) problems. However, readily available built-in material models found in these general-purpose FE

[1]Highway Engineer, Indiana Dept. of Transportation, 32 S. Broadway St., Greenfield, IN 46140. E-mail: mkim@indot.in.gov

[2]Associate Professor, Dept. of Civil and Environmental Engineering, Univ. of Illinois, 205 N. Mathews, Urbana, IL 61801 (corresponding author). E-mail: tutumlue@uiuc.edu

[3]Senior Pavement Engineer, Tensar International, 5883 Glenridge Dr., Suite 200, Atlanta, GA 30328. E-mail: jaykwon@tensarcorp.com

Note. This manuscript was submitted on March 30, 2007; approved on April 7, 2009; published online on September 15, 2009. Discussion period open until April 1, 2010; separate discussions must be submitted for individual papers. This paper is part of the ***International Journal of Geomechanics***, Vol. 9, No. 5, November 1, 2009. ©ASCE, ISSN 1532-3641/2009/5-195–208/$25.00.

programs are not in general applicable to the special nonlinear elastic, i.e., resilient response, analyses of pavement geomaterials.

This paper describes a recent pavement modeling research effort at the University of Illinois focused on incorporating proper characterizations of the nonlinear resilient behavior of the pavement foundation geomaterials into both axisymmetric and 3D FE analyses. The objective is to demonstrate how general-purpose FE programs should be used to suitably analyze flexible pavements by considering the nonlinear stress-dependent geomaterial behavior in order to more accurately predict pavement responses, which is essential in the framework of a mechanistic-empirical pavement design approach. Moreover, different resilient modulus models developed from true triaxial test data on unbound granular materials are also considered in modeling to properly account for the 3D stress states applied on cubical aggregate specimens. For this purpose, stress-dependent resilient modulus models, i.e., Uzan model (Uzan 1985) and universal octahedral shear stress model (Witczak and Uzan 1988) for base/subbase and bilinear model (Thompson and Robnett 1979) for subgrade, are programmed in a *user material subroutine* (UMAT) of ABAQUS FE program (Hibbit, Karlsson, & Sorensen, Inc. 2005). The Uzan model assumes the intermediate principal stress (σ_2) to be the same with the minor principal stress (σ_3) in the axisymmetric FE analyses. The universal model, on the other hand, can separately take into account the major, intermediate, and the minor principal stresses in both axisymmetric and 3D FE resilient response analyses for base layers. The GT-PAVE axisymmetric pavement analysis solutions are first used to verify the nonlinear UMAT subroutine predictions. The prediction ability of the developed nonlinear UMAT characterization is then validated by predicting similar pavement critical responses to those measured from field instrumented pavement test sections. Comparisons are made between axisymmetric and 3D analysis results emphasizing the importance of nonlinear geomaterial characterizations on the predicted critical pavement responses in contrast to linear elastic results. Comparisons are also made between axisymmetric and 3D FE analysis results emphasizing the effects of different nonlinear geomaterial model characterizations on the predicted critical pavement responses.

Nonlinear Stress-Dependent Geomaterial Models

Under the repeated application of traffic loads, most of the pavement deformations are recoverable and thus considered elastic. This is because after the material shakedown is reached during construction and initial trafficking with a certain number of load repetitions applied, the amount of permanent deformation in each load application decreases to a minimum. It has been customary to use resilient modulus (M_R) for the elastic stiffness of the pavement materials. M_R is defined as the repeatedly applied wheel load stress or deviator stress, σ_d, divided by the recoverable strain, ε_r, given by $M_R=\sigma_d/\varepsilon_r$. Repeated load triaxial tests are commonly employed to evaluate the resilient modulus of unbound aggregate and cohesive subgrade soils. Emphasis should be given in structural pavement analysis to realistic nonlinear material modeling in the base/subbase and subgrade layers based on repeated load triaxial test results.

The M_R in unbound granular base and often fine-grained subgrade has well known to be dependent on the current material stress state to which each pavement element is subjected. Since the stress states vary within a layer, moduli also change with both depth and horizontal distance. Therefore, layer modulus distributions should be predicted as a function of stress states for the most accurate pavement mechanistic analysis. This gives modulus distributions in accordance with stress distributions or stress bulbs in the layer and are much different from the single modulus assignment to the entire layer, such as in the linear elastic layered solutions. Furthermore, single modulus assignment also causes large horizontal tensile stresses to be predicted in aggregate base layers, which is in contradiction with the limited tension taking ability of aggregate materials.

Especially, an Uzan type model (Uzan 1985) considers the effects of both the confining and wheel load deviator stresses and thus handles very well the modulus variations in an unbound aggregate base layer. The Uzan model used to predict the typical stress-hardening behavior of unbound aggregate materials in axisymmetric FE analysis is given as follows:

$$M_R = K_1\left(\frac{\theta}{p_0}\right)^{K_2}\left(\frac{\sigma_d}{p_0}\right)^{K_3} \tag{1}$$

where bulk stress $\theta=\sigma_1+\sigma_2+\sigma_3=\sigma_1+2\sigma_3$; deviator stress $\sigma_d=\sigma_1-\sigma_3$; σ_1=total vertical stress; σ_3=confining (cell) pressure; p_0=unit pressure; and K_1, K_2, and K_3=constants or parameters from multiple regression analyses of the repeated load triaxial test data.

Later on, Witczak and Uzan (1988) proposed the use of a universal model developed from the Uzan model (Uzan 1985) by replacing the deviator stress term with the octahedral shear stress (τ_{oct}). Since the universal octahedral shear stress model considers material characteristics in all three directions, i.e., *x*-, *y*-, and *z*-directions, this model is more suitable to 3D FE pavement analysis

$$M_R = K_1 p_a\left(\frac{I_1}{p_a}\right)^{K_2}\left(\frac{\tau_{oct}}{p_a}\right)^{K_2} \tag{2}$$

where first stress invariant $I_1=\theta=\sigma_1+\sigma_2+\sigma_3$; $\tau_{oct}=1/3[(\sigma_1-\sigma_2)^2+(\sigma_1-\sigma_3)^2+(\sigma_2-\sigma_3)^2]^{1/2}$; p_a=atmospheric pressure; and K_1, K_2, and K_3=multiple regression parameters.

According to the recent mechanistic-empirical pavement design guide (National Cooperative Highway Research Program 2004), a generalized constitutive model similar to the universal model (Witczak and Uzan 1988) was proposed for use in Level I analysis for the nonlinear stress-dependent modeling of both the unbound aggregates and fine-grained soils. The differences in material behavior predicted by both models were only found in the regression variables but not in the predicted M_R values. For this reason, both the universal and mechanistic-empirical pavement design guide models can predict pavement responses well in 3D FE analyses.

Typically, fine-grained soil moduli decrease in proportion to the increasing stress levels thus showing stress-softening type behavior. The constitutive relationships are primarily established between the resilient modulus and the deviator stress. For a fine-grained subgrade layer, the bilinear model (Thompson and Robnett 1979) has been the most commonly used resilient modulus model. This bilinear soil model used in the FE analyses is given as follows:

$$M_R = K_1 + K_3 \times (K_2 - \sigma_d) \quad \text{when} \quad \sigma_d \le K_2$$

$$M_R = K_1 - K_4 \times (\sigma_d - K_2) \quad \text{when} \quad \sigma_d \ge K_2 \tag{3}$$

where K_1, K_2, K_3, and K_4=model parameters obtained from regression analyses of the repeated load triaxial test data and σ_d=deviator stress. Representing the bilinear behavior, parameter K_1

Int. J. Geomech., 2009, 9(5): 195-208

is referred to as the breakpoint modulus E_{Ri}, which is a characteristic soil property.

Pavement Analysis Using General-Purpose Finite-Element Programs

Previous Pavement Studies Using General-Purpose Finite-Element Programs

The FE method has been used extensively to analyze multilayered pavement systems with the advantage of including advanced pavement material models in the solutions as opposed to the use of linear elastic layered programs. Several axisymmetric FE programs, such as ILLI-PAVE (Raad and Figueroa 1980) and GT-PAVE (Tutumluer 1995) developed specifically for pavement analyses, properly take into account nonlinear material characterizations of unbound aggregates and subgrade soils by the use of a direct secant stiffness iterative solution approach for defining M_R as a function of stress state. Both ILLI-PAVE and GT-PAVE solutions were reported to predict very similar pavement responses for the nonlinear isotropic pavement foundations (Garg et al. 1998).

More recently, with the advent of computers and the need for 3D analysis, many researchers have attempted to predict flexible pavement responses and performances through the use of built-in material models readily available with most of the general-purpose FE programs, such as ABAQUS, ADINA, and ANSYS (Schwartz 2002; Sukumaran et al. 2004; Saad et al. 2005). These programs also offer an interface to implement new material models through a user-defined material subroutine (UMAT), in case one needs to develop a particular material model for specific engineering behavior not provided in the FE program's material library (Hjelmstad and Taciroglu 2000).

Hjelmstad and Taciroglu (2000) used the general-purpose ABAQUS FE program for the nonlinear flexible pavement analysis through a user-defined material subroutine incorporating the Uzan model and K-θ model formulated as a function of not stress but strain states for the nonlinear behavior of an unbound aggregate base. Different from the Uzan (1985) model, the K-θ model, given by $M_R=K_1\theta^{K_2}$, relates the resilient modulus (M_R) to the bulk stress (first stress invariant I_1) raised to a power and does not consider the shear stress effects. The nonlinear solutions by Hjelmstad and Taciroglu (2000) often predicted high asphalt bending stresses. Substantially different granular base stresses and strains were also obtained from different nonlinear models, some of which also considered various no-tension analyses to correct for large lateral tensile stresses often predicted in the base layer. The developed coupled hyperelastic constitutive model was also used in combination with the no-tension approach to model granular materials, which eventually yielded better fits to the experimental data.

The ABAQUS FE program was used for pavement analysis by Schwartz (2002) who also employed the K-θ model in the base course by using this time the "*HYPOELASTIC material model" inputs in the ABAQUS 3D modeling framework. The secant resilient modulus values could not be directly used in nonlinear solutions but were numerically converted to tangent moduli for input as a function of the first stress invariant, I_1. A tension cutoff was also imposed by specifying a very small modulus for tensile I_1 values. Comparing the linear and nonlinear solutions, Schwartz (2002) reported that there were up to 25% and 20% differences between the maximum asphalt tensile stresses and strains, respectively; for the most extreme case and less than 5% differences of stresses and strains at the top of the subgrade and the surface deflections. He also noted that these differences would seem acceptable for practical design.

Sukumaran et al. (2004) presented 3D pavement analysis results using ABAQUS. The studied topics in modeling were construction of mesh, mesh refinement, element aspect ratios, and material nonlinearities. Granular materials were modeled using the Mohr-Coulomb material model, which is an elastoplastic model. Dupont clay was modeled using a von Mises plasticity model. Instead of conducting resilient response analyses, this study compared pavement performance predictions with the available failure data from the National Airport Pavement Test Facility (NAPTF) of the Federal Aviation Administration.

ADINA FE program was recently used by Saad et al. (2005) for dynamic response analysis of flexible pavement structures subjected to single wheel traffic loads in 3D FE modeling. The effects of elastoplasticity of the base material and strain-hardening stiffness behavior of the silty sand subgrade material on the dynamic response were investigated with the use of a linear elastic asphalt concrete (AC). The base material was analyzed as elastic isotropic, elastic cross anisotropic, and using the Drucker-Prager model (Zaghloul and White 1993; Liu et al. 1998) as a strong or weak base and the subgrade was simulated by the modified CamClay model (Desai and Siriwardane 1984). Several conclusions were drawn from different case studies. The linear elastic cross-anisotropic base behavior resulted in 4% increase in the fatigue strain and 3% increase in vertical surface deflection. Elastoplasticity of the base material caused an increase of 46% in the rutting strain, 28% in the maximum tensile fatigue strain at the bottom of the asphalt layer, and 30% in the maximum surface deflection. The subgrade elastoplasticity had little impact on the fatigue strain, which was less than 1%.

Several FE pavement modeling studies conducted by a number of researchers were reviewed. In these studies, base and subgrade layer materials were treated as either elastic materials or elastoplastic materials. Even when the nonlinear material model was considered especially in the 3D FE studies, proper stress-dependent modulus characterizations were still not employed. Based on mechanistic-empirical design methodologies, pavement analysis relies primarily on a fundamental modulus characterization of the individual pavement layers to determine the state of stress and predict pavement performance. When these base and subgrade materials are used as pavement layers, the layer stiffness, resilient modulus is a function of applied stress state as proven in laboratory studies (Brown and Pappin 1981; Uzan 1985; Thompson and Elliott 1985). Therefore, there is a need to develop a user-defined material model subroutine for general-purpose FE programs to make them suitable for nonlinear pavement analysis.

Nonlinear Geomaterial Subroutine for the ABAQUS Program

A user-defined material subroutine, widely known as a UMAT subroutine in ABAQUS, was developed in this study to facilitate a direct secant modulus iterative solution technique using the material stress state. Note that the secant modulus approach may not be used for predicting microcracking leading to softening and its effects on deformations and stresses. It is used only for the geomaterial behavior in the resilient state, which is considered elastic since deformations are mainly recoverable after many load cycles.

Int. J. Geomech., 2009, 9(5): 195-208

Thus, the general Hooke's law governing geomaterial stress-strain relations takes the following form for isotropic behavior:

$$\sigma_{ij} = \frac{\nu E}{(1+\nu)(1-2\nu)}\varepsilon_{kk}\delta_{ij} + \frac{E}{1+\nu}\varepsilon_{ij} \quad (4)$$

In this pavement application, Young's modulus (E) is replaced by the resilient modulus (M_R). Generally, when constitutive properties are updated at the integration points within each element, the element stiffness matrix, K^e, is computed using the constitutive relation matrix D. This matrix D is given as follows:

$$D = \frac{M_R}{(1+\nu)(1-2\nu)} \times \begin{bmatrix} 1-\nu & \nu & \nu & 0 & 0 & 0 \\ \nu & 1-\nu & \nu & 0 & 0 & 0 \\ \nu & \nu & 1-\nu & 0 & 0 & 0 \\ 0 & 0 & 0 & \frac{1-2\nu}{2} & 0 & 0 \\ 0 & 0 & 0 & 0 & \frac{1-2\nu}{2} & 0 \\ 0 & 0 & 0 & 0 & 0 & \frac{1-2\nu}{2} \end{bmatrix} \quad (5)$$

Nonlinear iterations need to be performed using the appropriate resilient modulus models to calculate the modulus corresponding to the current stress state. Due to the nature of the material models used, an iterative procedure which considered a direct secant stiffness approach was found to be necessary in the analysis with an incremental loading scheme (Raad and Figueroa 1980; Tutumluer 1995). This method is less complicated than other nonlinear solution techniques, but it is sophisticated enough to give good convergence of the iterations to find resilient modulus of both stress-hardening and stress-softening materials. In fact, Tutumluer (1995) indicated that this was the only approach that worked with guaranteed convergence using a moduli averaging scheme as follows:

$$M_R^j = (1-\lambda)M_R^{j-1} + \lambda M_{R\ \text{model}}^j \quad (6)$$

where M_R^j=new M_R to be used at the end of iteration number j; λ=damping factor between 0.0 and 1.0; $M_R^{j-1}=M_R$ used at the end of iteration number $j-1$; $M_{R\ \text{model}}^j=M_R$ computed from the model at the end of iteration number j. To force convergence in the nonlinear iterations, the damping factor λ often needs to be assigned constant values less than or equal to 0.3 (Tutumluer 1995), which was considered in this study for consistency in the solutions. Furthermore, due to the incremental loading scheme, the initial moduli assigned in the geomaterial layers in the beginning of the nonlinear analysis do not generally influence the convergence process. The computing time depends on the complexity of nonlinear pavement analysis and the number of nodes and elements used in the FE mesh. The computing time estimates of axisymmetric analysis using nonlinear base and nonlinear subgrade materials is less than 60 s. The 3D nonlinear analysis took more than 20,000 s.

Pavement Section Analysis Domain Size for Finite-Element Mesh Construction

According to the semiinfinite half-space assumptions in the layered elastic theory, the pavement structure extends to infinity in the horizontal and vertical directions. For this reason, it is essential to choose a domain size that gives the most accurate pavement responses from FE analysis especially for those hard-to-match surface deflections. Duncan et al. (1968) reported that reasonable pavement responses were obtained when the analysis boundary moved to 50 times the radius of circular loading area (R) in the vertical direction and 12-times R in the horizontal direction. Recently, Kim (2000) found that the influence of boundary truncation was negligible for domains larger than about 150 times R in the vertical direction.

After studying several different axisymmetric FE mesh domain sizes, the domain size of 140-times R in the vertical direction and 20-times R in the horizontal direction was found to give accurate results using the eight-node isoparametric quadrilateral elements when compared to the analytical solutions provided by the linear elastic layered program, KENLAYER (Huang 2004). To especially achieve accurate subgrade responses and surface deformations, such a large domain was needed in the vertical direction.

Fig. 1 shows the constructed FE meshes for the selected domain size of 140-times R in the vertical direction and 20-times R in the horizontal direction and their dimensions for both the axisymmetric and 3D analyses. A constructed axisymmetric finite-element mesh shown in Fig. 1 had 300 quadratic elements and 981 nodes, and the 3D mesh consisted of 15,168 20-noded hexahedron elements and 67,265 nodes. All vertical boundary nodes had roller supports with fixed boundary nodes used at the bottom. The wheel load was applied as a uniform pressure of 551 kPa (80 psi) over a circular area of 152-mm (6-in.) radius. Table 1 lists the three-layered conventional flexible pavement geometries and the material properties used in the axisymmetric linear elastic FE analyses conducted for the domain size study pavement response predictions. Predicted pavement surface deflections ($\delta_{surface}$) and certain critical pavement responses, i.e., vertical stress and strain on top of subgrade (σ_v and ε_v) and horizontal stress at the bottom of the AC layer (σ_h), are compared in Table 2 with the linear elastic KENLAYER closed-form solutions to give in general a very good agreement.

Further horizontal domain size studies conducted with the depth of FE mesh fixed at 140-times R gave quite accurate subgrade responses and surface deflections with less than 0.025 mm (1 mil) difference when compared to the analytical results. As the horizontal domain increased to in excess of 20-times R, the accuracy of the predicted surface deformations did not improve under the same loading. Therefore, the influence of boundary truncation was negligible for domains larger than 20-times R in the horizontal direction.

Effects of Nonlinear Pavement Foundation Behavior

ABAQUS UMAT Verifications with GT-PAVE Axisymmetric Nonlinear Finite-Element Analyses

To verify the developed ABAQUS UMAT subroutine nonlinear solutions in the base and subgrade layers, GT-PAVE and ABAQUS axisymmetric FE programs were used to predict and compare pavement responses. GT-PAVE (Tutumluer 1995) is a specific-purpose nonlinear pavement analysis FE program that incorporates the aforementioned nonlinear material models for unbound base/subbase and fine-grained subgrade soil. A conventional flexible pavement was analyzed as an axisymmetric solid consisting of linear AC and nonlinear elastic unbound base and subgrade layers in order to employ the nonlinear response

Int. J. Geomech., 2009, 9(5): 195-208

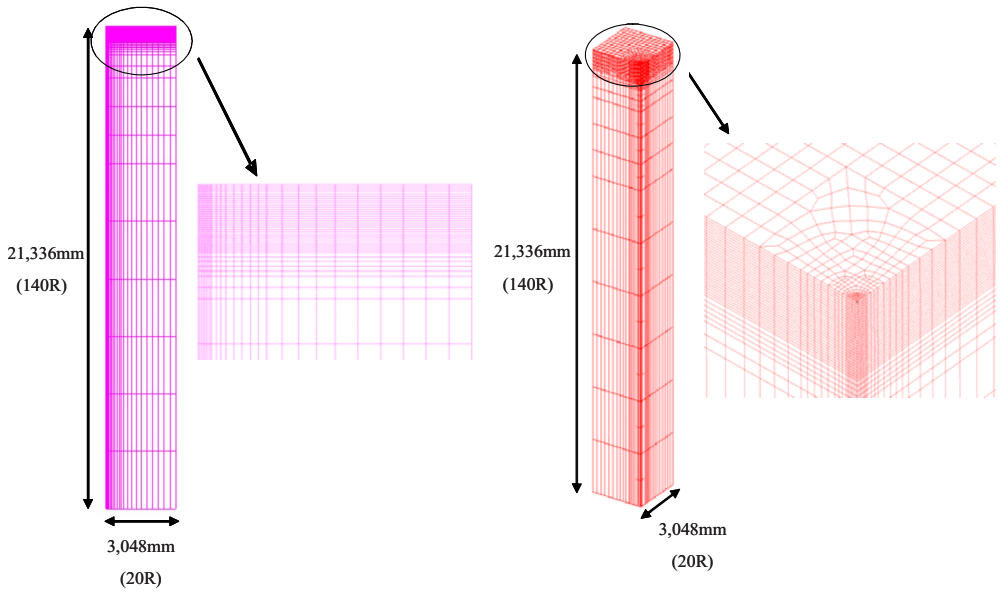

(a) Axisymmetric FE model (b) 3D FE model

Fig. 1. Typical axisymmetric and 3D FE meshes used for the selected domain size

models in the GT-PAVE and ABAQUS FE analyses. The pavement cross section consisted of 76 mm (3 in.) of AC, 305 mm (12 in.) of unbound aggregate base, and 8,865 mm (349 in.) deep fine-grained subgrade (Kim and Tutumluer 2006). Table 3 lists the material properties used in the nonlinear FE analyses. A rather high uniform pressure of 827 kPa (120 psi) was applied over a circular area with a radius of 102 mm (4 in.) to better contrast differences in results from the two FE program analyses and to compare them with the linear elastic solutions.

Table 4 presents the predicted critical pavement responses at the centerline of loading by the different combinations of GT-PAVE and ABAQUS FE linear and nonlinear analyses. Overall, the two nonlinear FE analysis programs are in very good agreement producing the same responses for each case the analysis results are compared thus verifying the applicability of the developed the ABAQUS UMAT subroutine to nonlinear pavement analysis. Fig. 2 shows, for nonlinear base and subgrade layers, very similar vertical stress distributions predicted at the centerline of loading (Kim and Tutumluer 2006). Similarly, Fig. 3 indicates good agreements even for the vertical resilient modulus distributions predicted by GT-PAVE and ABAQUS axisymmetric programs to further verify the nonlinear solution approach in the ABAQUS UMAT subroutine (Kim and Tutumluer 2006).

Comparisons of Axisymmetric Linear and Nonlinear Finite-Element Analyses

To better contrast the differences between the linear elastic solutions and the results of nonlinear pavement analyses, which consider the stress dependency of the base and subgrade materials, two different conventional flexible pavement geometries were selected for further analyses as follows:

- Pavement (1)—76 mm (3 in.) of AC and 305 mm (12 in.) of aggregate base.
- Pavement (2)—102 mm (4 in.) of AC and 254 mm (10 in.) of aggregate base.

The same material properties shown in Table 3 were assigned in these pavement sections for the layer properties. Accordingly, the Uzan model (Uzan 1985) was used in the base layer and the bilinear model (Thompson and Robnett 1979) was used in the subgrade layers with the model parameters given in Table 3. The FE structural analyses were conducted using the same mesh size with 140-times R in the vertical direction by 20-times R in the horizontal direction with 300 s order eight-node isoparametric quadrilateral elements used for a total of 981 nodes in the axisymmetric finite-element mesh, as shown in Fig. 1(a). A uniform pressure of 551 kPa (80 psi) was applied over the circular area of

Table 1. Selection of 140R (V) by 20R (H) Domain Size for Axisymmetric FE Analysis

Pavement geometry and material properties					
Layer	FE used	Thickness (mm)	E or M_R (MPa)	ν	Description of material properties
AC	Eight-noded quadrilateral	76	2,759	0.35	Isotropic and linear elastic
Base	Eight-noded quadrilateral	305	207	0.40	Isotropic and linear elastic
Subgrade	Eight-noded quadrilateral	20,955	41.4	0.45	Isotropic and linear elastic

Note: "R" stands for the radius of circular loading; "H" means in the horizontal direction; and "V" means in the vertical direction; 1 in. =25.4 mm; 1 ksi=6.89 MPa.

Int. J. Geomech., 2009, 9(5): 195-208

Table 2. Comparisons of Predicted Responses of Selected Domain Size Models

Pavement response (*tension is positive*)	Predicted pavement responses: KENLAYER	Predicted pavement responses: ABAQUS with eight-node quadrilateral elements
$\delta_{surface}$ (mm)	−0.927	−0.930
$\sigma_{h\ bottom\ of\ AC}$ (MPa)	0.777	0.773
$\sigma_{v\ top\ of\ subgrade}$ (MPa)	−0.041	−0.041
$\varepsilon_{v\ top\ of\ subgrade}$ ($\mu\varepsilon$)	−936	−933

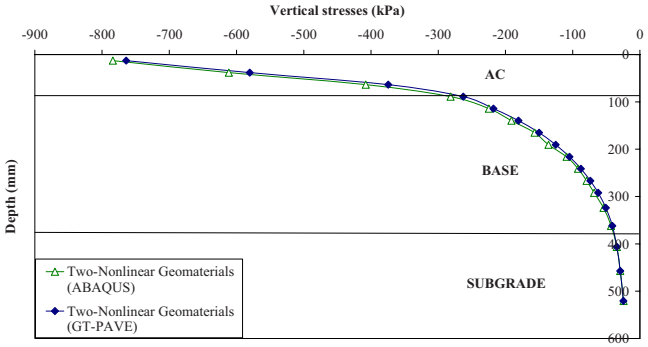

Fig. 2. Vertical stresses predicted by GT-PAVE and ABAQUS programs (Kim and Tutumluer 2006)

152-mm (6-in.) radius. Pavement responses were predicted from the axisymmetric ABAQUS FE analyses; all using the linear elastic AC material properties and the following pavement layer characterizations: (1) linear elastic; (2) nonlinear base and linear subgrade; (3) linear base and nonlinear subgrade; and finally, (4) nonlinear base and nonlinear subgrade. The linear elastic constant moduli assigned in the base and subgrade layers were determined based on the average modulus values obtained from the nonlinear analyses at the centerline of wheel loading. Note that such an assignment of equivalent linear modulus to the whole layer may result in a stiffer layer since the average layer modulus is the highest at the centerline of loading than in locations radially away. Nevertheless, such assignments are very common in multilayered linear elastic analyses of pavement structures. Especially, thin AC surfaced pavements for low volume roads were considered here to represent the more drastic influence of nonlinear resilient behavior in the base and subgrade layers. However, accounting properly for the nonlinear stress-dependent behavior is still important in thicker AC surfaced somewhat moderate to high volume highway pavements and flexible airport pavements since they are applied heavier wheel loads and are prone to rut accumulations in the granular base/subbase and subgrade layers.

Table 5 gives detailed comparisons of the predicted critical pavement responses for the two pavement geometry Cases (1) and (2) studied. The nonlinear base characterizations using the Uzan model had a remarkable effect on critical pavement responses, i.e., horizontal tensile strain (ε_h) at the bottom of AC and (ε_v) vertical strain on top of the subgrade. In comparison to linear elastic results, the nonlinear characterizations of the base caused maximum increases of 29% for the horizontal tensile strain (ε_h), 29% for the vertical strain (ε_v), and 33% for the surface deflection (δ). In addition, the nonlinearity of the subgrade also affected the critical pavement responses but this time in a negative fashion. In comparison to linear elastic results, the subgrade nonlinear characterizations using the bilinear model resulted in a maximum of 19% decrease in the vertical strain (ε_v) and 21% decrease in the surface deflection (δ). On the other hand, the nonlinearity of the

Table 3. Pavement Geometries and Material Properties in the Axisymmetric FE Analyses

Pavement layer	FE used	Thickness (mm)	E or M_R (MPa)	ν	Material properties					
AC	Eight-noded quadrilateral	76 or 102	2,759	0.35	Isotropic and linear elastic					
Base	Eight-noded quadrilateral	254 or 305	Nonlinear	0.40	Nonlinear: Uzan model [Eq. (1)]					
					K_1 (MPa)	K_2	K_3			
					4.1	0.64	0.065			
Subgrade	Eight-noded quadrilateral		Nonlinear	0.45	Nonlinear: bilinear model [Eq. (3)]					
					$K_1=E_{Ri}$ (MPa)	$K_2=\sigma_{di}$ (MPa)	K_3 (MPa/ MPa)	K_4 (MPa/ MPa)	σ_{dll} lower limit (MPa)	σ_{dul} upper limit (MPa)
					41.4	0.041	1,000	200	0.014	0.145

Note: 1 in.=25.4 mm; 1 ksi=6.89 MPa.

Table 4. Predicted Pavement Responses by ABAQUS and GT-PAVE Nonlinear Analyses

Pavement responses (*tension is positive*)	Nonlinear base and linear subgrade: GT-PAVE	Nonlinear base and linear subgrade: ABAQUS	Linear base and nonlinear subgrade: GT-PAVE	Linear base and nonlinear subgrade: ABAQUS	Nonlinear base and nonlinear subgrade: GT-PAVE	Nonlinear base and nonlinear subgrade: ABAQUS
$\delta_{surface}$ (mm)	−0.886	−0.884	−0.571	−0.569	−0.711	−0.716
$\delta_{top\ of\ subgrade}$ (mm)	−0.559	−0.559	−0.335	−0.333	−0.424	−0.426
$\varepsilon_{r\ bottom\ of\ AC}$ ($\mu\varepsilon$)	332	323	267	267	306	297
$\sigma_{v\ top\ of\ subgrade}$ (MPa)	−0.032	−0.033	−0.033	−0.033	−0.034	−0.034
$\varepsilon_{v\ top\ of\ subgrade}$ ($\mu\varepsilon$)	−830	−836	−530	−525	−674	−681

Note: 1 in.=25.4 mm; 1 ksi=6.89 MPa.

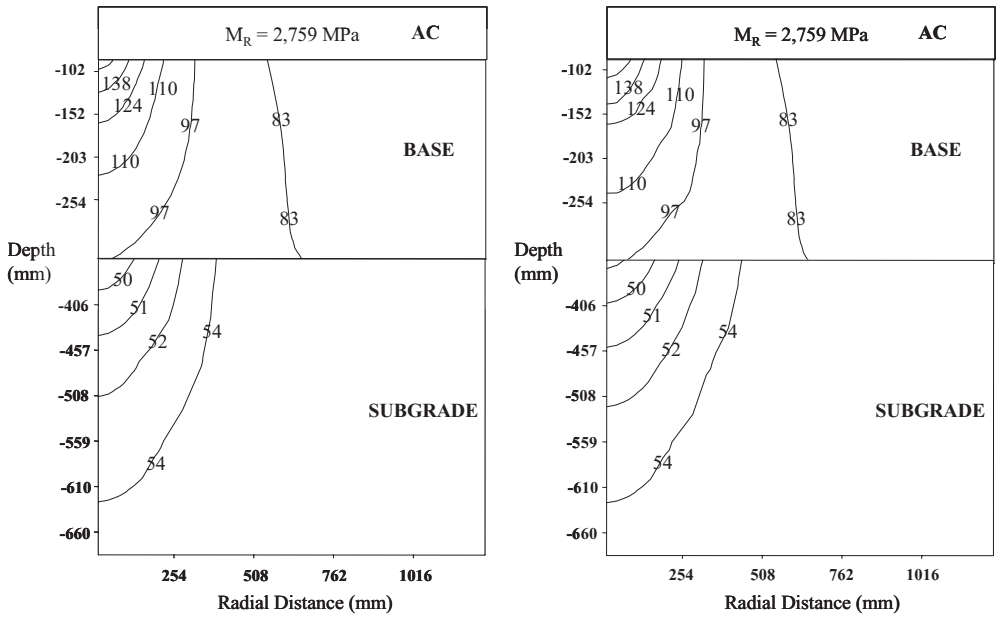

Fig. 3. Contours of vertical resilient modulus predicted by GT-PAVE and ABAQUS programs (Kim and Tutumluer 2006)

subgrade had in general very little impact on the tensile strains (ε_h) at the bottom of AC. For the combined nonlinear base and subgrade characterizations, the most accurate pavement responses, still considerably different from the linear elastic solutions, were predicted especially for the horizontal tensile strain (ε_h) at the bottom of AC and the vertical strain (ε_v) on top of the subgrade. Note that these differences in pavement responses, in these cases specific to the pavement geometries, layer material properties and the loading condition considered were contrasted to demonstrate the important effects of nonlinear pavement foundation modeling. It is very likely that when a higher level of nonlinearity exists, for example, due to a high quality crushed stone or a soft moisture-sensitive fine-grained subgrade soil, larger differences may be expected between the results of linear and nonlinear pavement comparative analyses.

Construction of Axisymmetric and Three-Dimensional Finite-Element Models and Mesh Equivalencies

Axisymmetric stress analysis is known to be limited in its capacity especially for modeling different geometries, such as, for a pavement interlayer or reinforcement having anisotropic properties on the horizontal plane and loading conditions related to multiple wheel/gear loading cases, which do not fit with the assumptions of axial symmetry. 3D FE analysis is viewed as the most advanced approach to eliminate such limitations and shortcomings with the consideration of all three-directional components, i.e., *x*-, *y*-, and *z*-directions. However, the accuracy of 3D FE analysis is dependent on the mesh refinement and mesh construction dealing with certain element aspect ratios. Smooth transitioning of FEs is also an important factor. Particularly, the mesh

Table 5. Comparisons of Predicted Critical Pavement Responses from Axisymmetric Linear and Nonlinear FE Analyses

Pavement responses (*tension is positive*)	Linear[b] elastic	Nonlinear base and linear subgrade	Linear base and nonlinear subgrade	Nonlinear base and nonlinear subgrade
Pavement (1): 76-mm AC and 305-mm base section				
δ surface (mm)	−0.930	−1.240 (+33.33%) [a]	−0.757 (−18.60%)[a]	−0.968 (+4.09%) [a]
$\varepsilon_{h\ \text{bottom of AC}}$ ($\mu\varepsilon$)	227	267 (+17.62%) [a]	227 (0%)[a]	257 (+13.22%) [a]
$\varepsilon_{v\ \text{top of subgrade}}$ ($\mu\varepsilon$)	−933	−1,203 (+28.94%) [a]	−772 (−17.26%)[a]	−937 (+0.43%) [a]
Pavement (2): 102-mm AC and 254-mm base section				
Pavement responses (*tension is positive*)	Linear elastic	Nonlinear base and linear subgrade	Linear base and nonlinear subgrade	Nonlinear base and nonlinear subgrade
δ surface (mm)	−0.866	−1.112 (+28.41%) [a]	−0.688 (−20.55%)[a]	−0.864 (−0.23%)[a]
$\varepsilon_{h\ \text{bottom of AC}}$ ($\mu\varepsilon$)	240	310 (+29.17%) [a]	234 (−2.50%)[a]	292 (+21.67%) [a]
$\varepsilon_{v\ \text{top of subgrade}}$ ($\mu\varepsilon$)	−896	−1,090 (+21.65%) [a]	−730 (−18.53%)[a]	−837 (−6.58%)[a]

Note: 1 in.=25.4 mm.

[a]The percentage value in the parenthesis indicates change from the linear elastic result.

[b]Based on the average constant moduli obtained from nonlinear analyses at the centerline of loading.

Int. J. Geomech., 2009, 9(5): 195-208

Table 6. Linear Elastic Analysis Results from Axisymmetric and 3D FE Meshes

Pavement response (*tension is positive*)	Linear elastic analyses: Axisymmetric FE model	3D FE model	Difference (%)
$\delta_{surface}$ (mm)	−0.930	−0.909	2.26
$\delta_{top\ of\ subgrade}$ (mm)	−0.683	−0.660	3.37
$\delta_{h\ bottom\ of\ AC}$ (MPa)	0.773	0.770	0.39
$\sigma_{v\ top\ of\ subgrade}$ (MPa)	−0.041	−0.040	2.44
$\varepsilon_{v\ top\ of\ subgrade}$ ($\mu\varepsilon$)	−933	−930	0.32

Note: 1 in.=25.4 mm; 1 ksi=6.89 MPa.

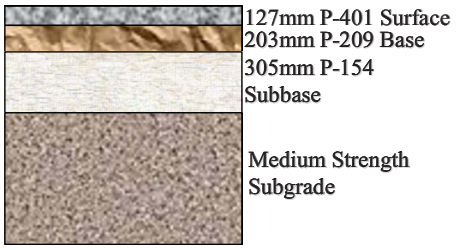

Fig. 4. Cross section of the NAPTF MFC pavement test section (Gopalakrishnan 2004)

generation for 3D FE pavement models has been problematic because the applied wheel load is localized and each pavement layer is relatively thin compared to the infinite domain. Therefore, neatly and well constructed meshes are necessary for proper 3D FE pavement analyses.

The generated 3D FE mesh, consisting of 15,168 20-noded hexahedron elements and 67,265 nodes, is shown in Fig. 1(b). The area subjected to wheel loading had a finer mesh to simulate an almost perfectly circular loading region, which gradually transitioned into to a square mesh construction. The lateral remote boundaries were truncated at a distance of 3,048 mm (120 in.), 20-times R away from the center of the loading, and the total depth of the pavement structure was taken as 21,336 mm (840 in.), 140-times R.

To verify the accuracy of the 3D FE pavement model, the linear elastic solutions were first obtained from both the ABAQUS axisymmetric and the 3D FE analyses. Like in the axisymmetric cases, a uniform pressure of 551 kPa (80 psi) was applied in the 3D FE analyses over the circular area of 152-mm (6-in.) radius. The pavement geometry and the linear elastic layer input properties listed in Table 1 were also assigned in this study with the exception of the 20-noded solid elements used in the 3D FE analysis instead of the eight-noded quadrilateral elements. Results are summarized in Table 6 to show the differences in predicted responses between the axisymmetric and 3D analyses for the linear elastic case studied. Overall, the differences in predicted pavement responses are quite small with the largest being for the surface deflection not more than 3%. Some of the critical pavement responses, such as the horizontal tensile stress (σ_h) at the bottom of AC and vertical strain (ε_v) on top of subgrade are even less than 1%. These comparisons between the axisymmetric and the 3D analyses are in general quite acceptable especially when considering all the assumptions made in the axisymmetric FE formulations and the circular shaped mesh discretization concerns for the wheel loading. Therefore, the developed 3D FE model was deemed accurate enough to study next the nonlinear pavement foundation modeling concepts in 3D FE analysis of flexible pavements.

Field Validation of Nonlinear Finite-Element Analysis Solutions

Field validation of the nonlinear stress-dependent geomaterial models programmed in to the UMAT subroutine was accomplished by computing nonlinear FE analysis results and comparing predictions to the field measured pavement responses of the NAPTF traffic testing (Gopalakrishnan 2004). Multidepth deflectometers (MDDs) and pressure cells (PCs) were installed in the test sections to measure the NAPTF pavement structural responses. The first built test sections, named as Construction Cycle 1 (CC1) included nine test pavements and the structural view of the medium, flexible and conventional (MFC) (conventional flexible pavement resting on a medium strength subgrade) section used in the validation study is shown in Fig. 4.

The 3D FE analyses were performed to compute the pavement responses under aircraft gear/wheel loadings and compare them with the measured CC1 pavement test section responses of NAPTF. Table 7 lists the pavement layer thicknesses and material properties used in the validation study including the nonlinear resilient modulus model parameters of the unbound aggregates and subgrade materials used in the NAPTF MFC section. These results were used as inputs for performing 3D finite-element analyses.

Table 7. Pavement Geometries and Material Properties Used in the Field Validation Study

Pavement layer	FE used	Thickness (mm)	E or M_R (MPa)	ν	Material properties			
AC	20-noded hexahedron	127	8,268	0.35	Isotropic and linear elastic			
Base	20-noded hexahedron	203	Nonlinear	0.38	Nonlinear: Uzan model [Eq. (1)]			
					K_1 (MPa)		K_2	K_3
					10.3		0.40	0
Subbase	20-noded hexahedron	305	Nonlinear	0.38	Nonlinear: Uzan model [Eq. (1)]			
					K_1 (MPa)		K_2	K_3
					6.9		0.64	0
Subgrade	20-noded hexahedron		Nonlinear	0.40	Nonlinear: bilinear model [Eq. (3)]			
					$K_1=E_{Ri}$ (MPa)	$K_2=\sigma_{di}$ (MPa)	K_3	K_4
					62.8	0.042	420	570

Note: 1 in.=25.4 mm; 1 ksi=6.89 MPa.

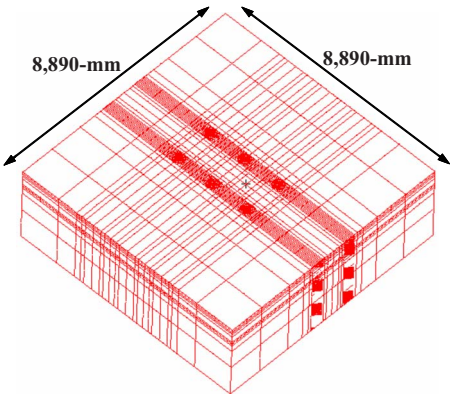

Fig. 5. 3D FE mesh used in the field validation study

The 3D FE model geometry used to analyze the MFC section is shown in Fig. 5. All elements used were parabolic 20-noded hexahedron solid elements. A constructed 3D mesh consisted 18,719 20-noded hexahedron elements and 47,371 nodes. All vertical boundary nodes had roller supports with fixed horizontal boundary nodes used at the bottom. The subgrade and the unbound aggregate base layers were treated as nonlinear elastic materials while the AC surface layer was modeled as linear elastic. To model the MFC test section, individual wheel loads were approximated as a uniform pressure applied over a circular area shown in Fig. 5. A six-wheel dual-tridem type aircraft gear configuration applied individual wheel loads of 20 t (uniform tire pressure of 1.3 MPa) with a 1,372-mm wheel spacing and a 1,448-mm axle spacing.

Fig. 6(a) shows predicted subgrade vertical stresses comparable in magnitudes to those measured by the PCs in the longitudinal loading direction. In each test section, four PCs were installed on top of the subgrade to measure the vertical stresses. However, data were not available for all four PCs in most cases like in the MFC section. The measured PC results showed large variability possibly due to the differences in the actual installation depths of the PCs. Also, the measured MDD deflections in the transverse direction are shown in Figs. 6(b and c) to compare favorably with the FE predictions.

From the comparisons, the nonlinear FE mechanistic model predictions showed generally good agreement with the measured responses of the NAPTF MFC test section. The predicted values of subgrade vertical stress, surface displacement, and subgrade displacement compared reasonably well with the order of magnitudes of the measured responses in the MFC section.

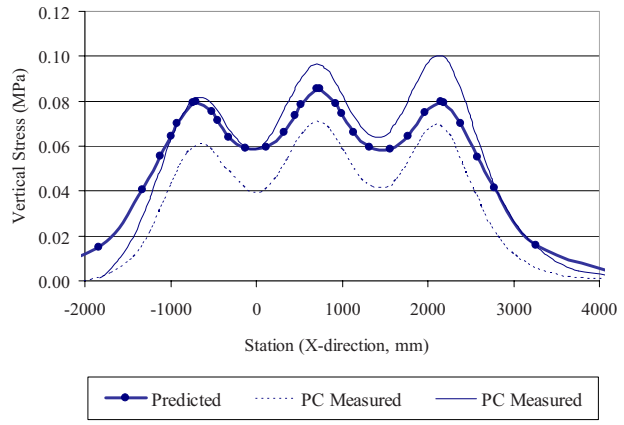

(a) Predicted and pressure cell (PC) measured subgrade stresses

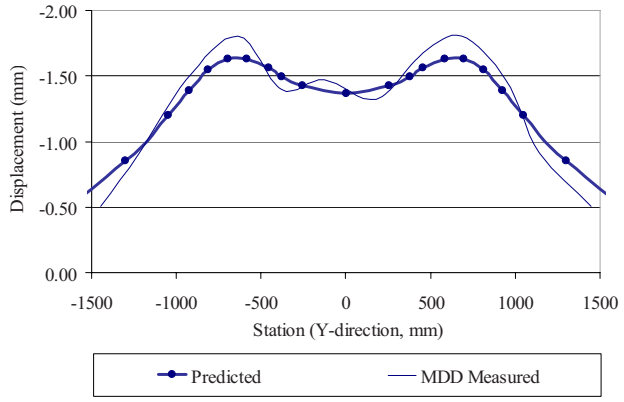

(b) Predicted and MDD measured surface displacements

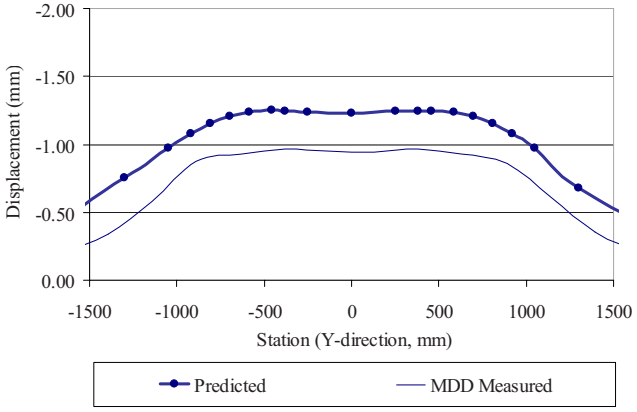

(c) Predicted and MDD measured subgrade displacements

Fig. 6. Comparisons between measured and FE predicted responses for the NAPTF MFC test section

True Triaxial Tests on Unbound Granular Materials

Although 3D nonlinear FE analysis of flexible pavements is currently the state-of-the-art structural analysis approach, most stress-dependent characterization models used in the nonlinear analyses are commonly developed from repeated load triaxial tests, primarily designed for the axisymmetric stress analysis. That is, under triaxial conditions with $\sigma_2=\sigma_3$, no consideration is given to having an applied intermediate principal stress (σ_2) different than the minor principal stress σ_3. This makes axisymmetric stress analysis limited in its capacity for modeling actual field geometries and loading conditions, such as multiple wheel/gear loading scenarios, and the needed upgrade to the state-of-the-art 3D FE analyses of flexible pavements should properly consider 3D stress states in the implementation of the nonlinear pavement foundation geomaterial behavior.

Nonlinear Models Developed from True Triaxial Tests

The limitation of a repeated load triaxial test, particularly its inability to simulate arbitrary applied stresses in three orthogonal directions, necessitates the use of a true triaxial device. Such a true triaxial test device was used recently by Rowshanzamir (1995) at the University of New South Wales and was capable of

Int. J. Geomech., 2009, 9(5): 195-208

Table 8. Aggregate Nonlinear Model Parameters Determined from the Test Data by Rowshanzamir (1995)

Model type	Model parameters			
	K_1	K_2	K_3	R^2 [a]
Eq. (1): Uzan model (with stress states from triaxial tests)	3,502	0.635	0.010	0.79
Eq. (2): universal model (with stress states from triaxial tests)	1,360	0.635	0.010	0.79
Eq. (2): universal model (with 3D stress states from true triaxial tests)	417	1.071	−0.107	0.98

[a]R^2=regression correlation coefficient.

dynamically applying 3D principal stresses on the faces of a 100-mm cubical aggregate specimen in a stress controlled cell. Repeated loads of up to 6 kN at frequencies ranging from 0.01 to 5 Hz were applied to the test specimen through a specially designed hydraulic system. To avoid the corner problem in the boundaries of the cubical device, a sliding spring was installed. Rowshanzamir (1995) used the true triaxial testing machine for determining the resilient properties of a base course granular material, well-graded crushed basalt, in the laboratory. The original laboratory data by Rowshanzamir (1995), consisting of applied stresses and measured strains from the tests, were used in this study to develop nonlinear stress-dependent models of the Uzan and the universal forms. Table 8 gives the resilient model parameters and regression results obtained using the true triaxial test data. The axisymmetric universal model was obtained by assuming intermediate principal stresses σ_2 equal to the applied σ_3 stresses in triaxial conditions. The lack of intermediate principal stresses was mainly the reason why the axisymmetric case characterization models gave lower R^2 correlation coefficients.

Comparisons of Nonlinear Pavement Responses Using Different Material Characterizations

With the stress-dependent base course resilient modulus (M_R) models developed using the true triaxial test data (Rowshanzamir 1995), various comparisons showing the effects of advanced testing and characterization on pavement response predictions could be made successfully. To perform 3D nonlinear FE analysis, the universal model given in Eq. (2) was used for the unbound aggregate base while the bilinear model was used in the fine-grained subgrade as the ABAQUS UMAT inputs in the 3D mesh [see Fig. 1(b)] with the assumption of linear elastic AC layer behavior. Table 9 lists the pavement geometries and the input material properties including nonlinear model parameters used in the 3D FE analyses. A uniform pressure of 551 kPa was applied over a circular area of a 152-mm radius. The FE mesh shown in Fig. 1 and the same wheel loading conditions were also used for the axisymmetric FE analyses, which employed eight-noded quadrilateral elements. Four different modeling cases using different base course characterizations were selected for studying as follows:

- **Case (1)**—Axisymmetric FE analysis using the Uzan model.
- **Case (2)**—Axisymmetric FE analysis using the universal model with triaxial $\sigma_2=\sigma_3$ assumption.
- **Case (3)**—3D FE analysis using the universal model with triaxial $\sigma_2=\sigma_3$ assumption.
- **Case (4)**—3D FE analysis using the universal model with all three stress components ($\sigma_2 \neq \sigma_3$) and τ_{oct}.

Tables 10–13 give detailed comparisons of the predicted critical pavement responses for two different pavement geometries: (1) 76-mm AC and 305-mm base; (2) 102-mm AC and 254-mm base. In all the nonlinear analyses, the bilinear M_R model was used in the subgrade layers. The predicted pavement responses were investigated in relation to different combinations of linear and nonlinear analyses in the base and subgrade: (1) nonlinear base and linear subgrade; (2) nonlinear base and nonlinear subgrade. By comparing responses predicted between Cases (2) and (3), mesh and geometry related differences between axisymmetric

Table 9. Pavement Geometries and Material Properties in the 3D Nonlinear FE Analyses

Pavement layer	FE used	Thickness (mm)	E or M_R (MPa)	ν	Material properties
AC	20-noded solid	76 or 102	2,759	0.35	Isotropic and linear elastic
Base	20-noded solid	254 or 305	Nonlinear	0.40	Nonlinear: Uzan model [Eq. (1)]
					K_1 (MPa) / K_2 / K_3: 3.5 / 0.635 / 0.010
					Nonlinear: universal model [Eq. (2)][a]
					K_1 / K_2 / K_3: 1,360 / 0.635 / 0.010
					Nonlinear: universal model [Eq. (2)][b]
					K_1 / K_2 / K_3: 417 / 1.071 / −0.107
Subgrade	20-noded solid	20,955 or 20,980	Nonlinear	0.45	Nonlinear: bilinear model [Eq. (3)]
					$K_1=E_{Ri}$ (MPa) / $K_2=\sigma_{di}$ (MPa) / K_3 (MPa/MPa) / K_4 (MPa/MPa) / σ_{dll} lower limit (MPa) / σ_{dul} upper limit (MPa): 41.4 / 0.041 / 1,000 / 200 / 0.014 / 0.145

Note: 1 in.=25.4 mm; 1 MPa=6.89 ksi.

[a]The resilient model considered triaxial conditions ($\sigma_2=\sigma_3$).

[b]The resilient model considered all three stress components.

Int. J. Geomech., 2009, 9(5): 195-208

Table 10. Comparisons of Predicted Pavement Responses from Cases (2) and (3)

	Nonlinear base and linear subgrade[a]		Nonlinear base and nonlinear subgrade[a]	
Pavement response	Axisymmetric (Case 2)	3D (Case 3)	Axisymmetric (Case 2)	3D (Case 3)
76-mm AC and 305-mm base section				
$\delta_{surface}$ (mm)	−1.102	−1.059 (−4)[b]	−0.859	−0.840 (−2)
$\sigma_{h\ \text{bottom of AC}}$ (MPa)	0.531	0.563 (+6)	0.517	0.547 (+6)
$\varepsilon_{h\ \text{bottom of AC}}$ ($\mu\varepsilon$)	192	196 (+2)	188	191 (+2)
$\sigma_{v\ \text{top of subgrade}}$ (MPa)	−0.059	−0.057 (−5)	−0.073	−0.070 (−4)
$\varepsilon_{v\ \text{top of subgrade}}$ ($\mu\varepsilon$)	−1,042	−974 (−7)	−818	−793 (−3)
102-mm AC and 254-mm base section				
$\delta_{surface}$ (mm)	−1.019	−0.978 (−4)	−0.787	−0.775 (−2)
$\sigma_{h\ \text{bottom of AC}}$ (MPa)	0.828	0.823 (−1)	0.789	0.819 (+4)
$\varepsilon_{h\ \text{bottom of AC}}$ ($\mu\varepsilon$)	245	240 (−2)	235	238 (+1)
$\sigma_{v\ \text{top of subgrade}}$ (MPa)	−0.055	−0.053 (−4)	−0.068	−0.067 (−2)
$\varepsilon_{v\ \text{top of subgrade}}$ ($\mu\varepsilon$)	−979	−922 (−6)	−769	−759 (−1)

[a]Tension is positive.

[b]The values in parentheses indicate percentage change from Case (2) to Case (3) results.

and 3D FE analyses could be realistically investigated. The effects of intermediate principal stress (σ_2) on nonlinear behavior could be studied by comparing results from Cases (3) and (4). By comparing axisymmetric and 3D analysis results from Cases (2) and (4), the limitations and applicability of triaxial testing and characterization could be investigated in 3D analyses. And finally, a comparison of Cases (1) and (4) would reflect the overall differences in results in an accumulated manner.

In Table 10, axisymmetric and 3D FE analysis results are compared for the same modulus models from triaxial testing. From both linear and nonlinear analyses considered in the subgrade and nonlinear behavior in the aggregate base, the 3D analysis results were not much different from those of the axisymmetric analyses with a largest difference of 7% for vertical strain (ε_v) on top of the subgrade. This indicated no major mesh or geometry related differences were found between axisymmetric and 3D analyses of the single wheel loading approximation.

The effects of intermediate principal stress (σ_2) are indicated in Table 11. The two FE models had the exact same 3D FE meshes and nonlinear material models with the only difference being the intermediate principal stress was replaced with the minor principal stress (σ_3) in finding the granular material model parameters of Case (3). The use of the true triaxial test data by Rowshanzamir (1995) made this comparison possible. The use of intermediate principal stress (σ_2) had the most impact on the horizontal strain and stress predictions at the bottom of AC as they showed the largest percent differences, up to 18% differences in the AC horizontal stresses.

Table 12 results summarize the combined effects of the applicability of triaxial testing/characterization and also the intermediate principal stress (σ_2) in 3D analyses. The horizontal strain and stress predictions at the bottom of AC again showed the largest percent differences between Cases (2) and (4) results. In addition, with the linear subgrade, vertical subgrade strains also indicated a difference of up to 8%, which could be mostly due to axisymmetric and 3D mesh differences (see Table 10).

Finally, Table 13 presents the most drastic results, i.e., highest percent differences, in the computed responses when predicted responses are compared between Cases (1) and (4). Note that this is often what most researchers studied and compared in the past, e.g., Schwartz (2002). These results agree well with the differences between the axisymmetric Uzan and 3D universal model

Table 11. Comparisons of Predicted Pavement Responses from Cases (3) and (4)

	Nonlinear base and linear subgrade[a]		Nonlinear base and nonlinear subgrade[a]	
Pavement response	3D (Case 3)	3D (Case 4)	3D (Case 3)	3D (Case 4)
76-mm AC and 305-mm base section				
$\delta_{surface}$ (mm)	−1.059	−1.061 (0)[b]	−0.840	−0.839 (0)
$\sigma_{h\ \text{bottom of AC}}$ (MPa)	0.563	0.464 (−18)	0.547	0.447 (−18)
$\varepsilon_{h\ \text{bottom of AC}}$ ($\mu\varepsilon$)	196	179 (−8)	191	175 (−9)
$\sigma_{v\ \text{top of subgrade}}$ (MPa)	−0.057	−0.058 (+3)	−0.070	−0.073 (+4)
$\varepsilon_{v\ \text{top of subgrade}}$ ($\mu\varepsilon$)	−974	−958 (−2)	−793	−789 (−1)
102-mm AC and 254-mm base section				
$\delta_{surface}$ (mm)	−0.978	−0.983 (+1)	−0.775	−0.782 (+1)
$\sigma_{h\ \text{bottom of AC}}$ (MPa)	0.823	0.727 (−12)	0.819	0.744 (−9)
$\varepsilon_{h\ \text{bottom of AC}}$ ($\mu\varepsilon$)	240	223 (−7)	238	227 (−5)
$\sigma_{v\ \text{top of subgrade}}$ (MPa)	−0.053	−0.054 (+3)	−0.067	−0.070 (+5)
$\varepsilon_{v\ \text{top of subgrade}}$ ($\mu\varepsilon$)	−922	−904 (−2)	−759	−765 (+1)

[a]Tension is positive.

[b]The values in parentheses indicate percentage change from Case (3) to Case (4) results.

Int. J. Geomech., 2009, 9(5): 195-208

FE analysis results in Cases (1) and (4). Since different models were used in the base layer with different axisymmetric and 3D stress states, the largest differences, up to 32% change in horizontal stress (σ_h) at the bottom of AC layer and 9% change in vertical strain (ε_v) on top of subgrade, occurred as shown in Table 13. Note that the results obtained from all different cases and analyses studied had compensating effects, positive and negative percent differences, on the computed critical pavement responses. When the fatigue life is considered, the number of load repetitions related to the differences in asphalt tensile strain will be very large.

Summary and Conclusions

To properly characterize the resilient response of geomaterials, i.e., coarse-grained unbound aggregates and fine-grained subgrade soils, appropriate stress-dependent modulus characterization models were programmed in a user-defined material model subroutine (UMAT) in the general-purpose ABAQUS FE program. This way, stress-dependent characterizations of the base and subgrade layers were made part of the ABAQUS FE nonlinear solutions. To converge smoothly in each loading, a direct secant stiffness approach was adopted in nonlinear analysis to work suitably for both ABAQUS axisymmetric and 3D flexible pavement response analyses.

Using closed-form linear elastic solutions, an axisymmetric FE mesh size was first selected for accurately predicting pavement responses, i.e., stress, strain, and deflection. The results of the nonlinear UMAT analyses were then verified with the axisymmetric GT-PAVE FE program pavement analysis results for a conventional flexible pavement section studied. Compared to the linear elastic solutions, i.e., one modulus assigned to the whole subgrade or base layer, significantly different critical pavement responses, e.g., horizontal tensile strain at bottom of AC linked to fatigue cracking and vertical strain on top of subgrade linked to rutting, were predicted when nonlinear analyses were performed in the aggregate base and fine-grained subgrade soil layers.

The investigation with the developed UMAT for the general-

Table 12. Comparisons of Predicted Pavement Responses from Cases (2) and (4)

	Nonlinear base and linear subgrade[a]		Nonlinear base and nonlinear subgrade[a]	
Pavement response	Axisymmetric (Case 2)	3D (Case 4)	Axisymmetric (Case 2)	3D (Case 4)
76-mm AC and 305-mm base section				
$\delta_{surface}$ (mm)	−1.102	−1.061 (−4)[b]	−0.859	−0.839 (−2)
$\sigma_{h\ bottom\ of\ AC}$ (MPa)	0.531	0.464 (−13)	0.517	0.447 (−14)
$\varepsilon_{h\ bottom\ of\ AC}$ ($\mu\varepsilon$)	192	179 (−7)	188	175 (−7)
$\sigma_{v\ top\ of\ subgrade}$ (MPa)	−0.059	−0.058 (−2)	−0.073	−0.073 (0)
$\varepsilon_{v\ top\ of\ subgrade}$ ($\mu\varepsilon$)	−1,042	−958 (−8)	−818	−789 (−4)
102-mm AC and 254-mm base section				
$\delta_{surface}$ (mm)	−1.019	−0.983 (−4)	−0.787	−0.782 (−1)
$\sigma_{h\ bottom\ of\ AC}$ (MPa)	0.828	0.727 (−12)	0.789	0.744 (−6)
$\varepsilon_{h\ bottom\ of\ AC}$ ($\mu\varepsilon$)	245	223 (−9)	235	227 (−3)
$\sigma_{v\ top\ of\ subgrade}$ (MPa)	−0.055	−0.054 (−1)	−0.068	−0.070 (+3)
$\varepsilon_{v\ top\ of\ subgrade}$ ($\mu\varepsilon$)	−979	−904 (−8)	−769	−765 (−1)

[a]Tension is positive.

[b]The values in parentheses indicate percentage change from Case (2) to Case (4) results.

Table 13. Comparisons of Predicted Pavement Responses from Cases (1) and (4)

	Nonlinear base and linear subgrade[a]		Nonlinear base and nonlinear subgrade[a]	
Pavement response	Axisymmetric (Case1)	3D (Case 4)	Axisymmetric (Case1)	3D (Case 4)
76-mm AC and 305-mm base section				
$\delta_{surface}$ (mm)	−1.130	−1.061 (−6)[b]	−0.886	−0.839 (−5)
$\sigma_{h\ bottom\ of\ AC}$ (MPa)	0.665	0.464 (−30)	0.654	0.447 (−32)
$\varepsilon_{h\ bottom\ of\ AC}$ ($\mu\varepsilon$)	219	179 (−18)	215	175 (−19)
$\sigma_{v\ top\ of\ subgrade}$ (MPa)	−0.060	−0.058 (−2)	−0.073	−0.073 (0)
$\varepsilon_{v\ top\ of\ subgrade}$ ($\mu\varepsilon$)	−1,047	−958 (−9)	−840	−789 (−6)
102-mm AC and 254-mm base section				
$\delta_{surface}$ (mm)	−1.039	−0.983 (−5)	−0.805	−0.782 (−3)
$\sigma_{h\ bottom\ of\ AC}$ (MPa)	0.952	0.727 (−24)	0.908	0.744 (−18)
$\varepsilon_{h\ bottom\ of\ AC}$ ($\mu\varepsilon$)	268	223 (−17)	257	227 (−12)
$\sigma_{v\ top\ of\ subgrade}$ (MPa)	−0.055	−0.054 (−1)	−0.067	−0.070 (+5)
$\varepsilon_{v\ top\ of\ subgrade}$ ($\mu\varepsilon$)	−988	−904 (−9)	−784	−765 (−2)

[a]Tension is positive.

[b]The values in parentheses indicate percentage change from Case (1) to Case (4) results.

Int. J. Geomech., 2009, 9(5): 195-208

purpose FE programs proved that 3D nonlinear flexible pavement analyses could be accurately performed in the case of multiple wheel/gear loading applied on a flexible airport pavement test section. The predicted pavement responses matched closely with the displacements and stresses measured in the field and the 3D FE analyses could be reasonably applied to the design of airfield pavements serving multiple wheel gear loads when the nonlinear pavement geomaterials were considered.

For evaluating the impacts of triaxial and true triaxial testing options in the laboratory on the stress-dependent modulus model characterizations, the most realistic true triaxial test data for unbound aggregate base materials were used as obtained from a previous study. Several comparative analyses were undertaken to study the effects of axisymmetric and 3D FE analyses for a single wheel loading approximation and the consideration of the intermediate principal stress (σ_2). In the comparison of axisymmetric and 3D FE results, both linear and nonlinear analyses showed no significant differences only when the exact same modulus characterization models defined from axisymmetric stress conditions were used in both analyses. The largest and the most drastic differences were obtained when comparing responses predicted from the axisymmetric and 3D nonlinear FE analyses using just the Uzan model developed from triaxial test data with the triaxial assumption of equal minor and intermediate stresses ($\sigma_2=\sigma_3$) and the universal model for 3D analysis employing additional intermediate stress (σ_2) and the octahedral shear stress (τ_{oct}) instead of the deviator stress (σ_d) for shear stress effects. Somewhat lower AC horizontal strain and stress responses were predicted from 3D analyses. This means neglecting σ_2 in the axisymmetric solutions may be somewhat conservative for flexible pavement AC fatigue predictions.

Notation

The following symbols are used in this paper:

D = constitutive relation matrix;
E = Young's modulus;
I_1 = stress invariant;
K^e = element stiffness matrix;
K_1, K_2, K_3, and K_4 = constants or parameters from multiple regression analyses of the repeated load triaxial test data;
M_R = resilient modulus;
M_R^j = new M_R to be used at the end of iteration number j;
M_R^{j-1} = M_R used at the end of iteration number $j-1$;
$M_{R\ \mathrm{model}}^j$ = M_R computed from the model at the end of iteration number j;
p_a = atmospheric pressure;
p_0 = unit pressure;
δ_{ij} = Kronecker delta;
ε_{ij} = strain tensor;
ε_{kk} = volumetric strain;
ε_r = recoverable strain;
θ = total vertical stress, bulk stress, the first stress invariant ($\sigma_1+\sigma_2+\sigma_3=\sigma_1+2\sigma_3$);
σ_d = deviator stress ($\sigma_1-\sigma_3$);
σ_2 = intermediate principal stress;
σ_3 = minor principal stress, confining (cell) pressure;
σ_{ij} = stress tensor;
τ_{oct} = octahedral shear stress $[1/3[(\sigma_1-\sigma_2)^2+(\sigma_1-\sigma_3)^2+(\sigma_2-\sigma_3)^2]^{1/2}]$;
ν = Poisson's ratio; and
λ = damping factor between 0.0 and 1.0.

References

Brown, S. F., and Pappin, J. W. (1981). "Analysis of pavements with granular bases." *Transportation Research Record. 810*, Transportation Research Board, Washington, D.C., 17–23.

Desai, C. S., and Siriwardane, H. J. (1984). *Constitutive laws for engineering materials*, Prentice-Hall, Englewood Cliffs, N.J.

Duncan, J. M., Monismith, C. L., and Wilson, E. L. (1968). "Finite element analyses of pavements." *Transportation Research Record. 228*, Transportation Research Board, Washington, D.C., 18–33.

Garg, N., Tutumluer, E., and Thompson, M. R. (1998). "Structural modeling concepts for the design of airport pavements for heavy aircraft." *Proc., 5th Int. Conf. on the Bearing Capacity of Roads and Airfields*, Trondheim, Norway, 115–124.

Gopalakrishnan, K. (2004). "Performance analysis of airport flexible pavements subjected to new generation aircraft." Ph.D. dissertation, Univ. of Illinois, Champaign, Ill.

Hibbit, Karlsson, & Sorensen, Inc. (2005). *ABAQUS/standard user's manual, version 6.5*, Hibbit, Karlsson, & Sorensen, Pawtucket, R.I.

Hjelmstad, K. D., and Taciroglu, E. (2000). "Analysis and implementation of resilient modulus models for granular solids." *J. Eng. Mech.*, 126(8), 821–830.

Huang, Y. H. (2004). *Pavement analysis and design*, 2nd Ed., Prentice-Hall, Upper Saddle River, N.J.

Kim, J. (2000). "Three-dimensional finite element analysis of multilayered systems." Ph.D. dissertation, Univ. of Illinois, Champaign, Ill.

Kim, M., and Tutumluer, E. (2006). "Modeling nonlinear, stress dependent pavement foundation behavior using a general-purpose finite element program." *ASCE Geotechnical Special Publication No. 154, Pavement Mechanics and Performance*, B. Huang, R. Meier, J. Prozzi, and E. Tutumluer, eds., 29–36.

Liu, X., Scarpas, A., Blaauwendraad, J., and Genske, D. D. (1998). "Geogrid reinforcing of recycled aggregate materials for road construction: Finite element investigation." *Transportation Research Record. 1611*, Transportation Research Board, Washington, D.C., 78–85.

National Cooperative Highway Research Program 1-37A. (2004). "Guide for mechanistic-empirical design of new and rehabilitated pavement structures." *Final Rep.*, TRB, National Research Council, Washington, D.C., ⟨http://www.trb.org/mepdg/home.htm⟩.

Raad, L., and Figueroa, J. L. (1980). "Load response of transportation support systems." *Transp. Engrg. J.*, 106(1), 111–128.

Rowshanzamir, M. A. (1995). "Resilient cross-anisotropic behavior of granular base materials under repetitive loading." Ph.D. dissertation, School of Civil Engineering, Univ. of New South Wales, Kensington, Australia.

Saad, B., Mitri, H., and Poorooshasb, H. (2005). "Three-dimensional dynamic analysis of flexible conventional pavement foundation." *J. Transp. Eng.*, 131(6), 460–469.

Schwartz, C. W. (2002). "Effect of stress-dependent base layer on the superposition of flexible pavement solutions." *Int. J. Geomech.*, 2(3), 331–352.

Sukumaran, B., Chamala, N., Willis, M., Davis, J., Jurewicz, S., and Kyatham, V. (2004). "Three dimensional finite element modeling of flexible pavements." *Proc., 2004 FAA Worldwide Airport Technology Transfer Conf.*, Atlantic City, N.J.

Thompson, M. R., and Elliott, R. P. (1985). "ILLI-PAVE based response algorithms for design of conventional flexible pavements." *Transportation Research Record. 1043*, Transportation Research Board, Washington, D.C., 50–57.

Thompson, M. R., and Robnett, Q. L. (1979). "Resilient properties of

subgrade soils." *Transp. Engrg. J.*, 105(1), 71–89.
Tutumluer, E. (1995). "Predicting behavior of flexible pavements with granular bases." Ph.D. dissertation, School of Civil and Environmental Engineering, Georgia Institute of Technology, Atlanta.
Uzan, J. (1985). "Characterization of granular materials." *Transportation Research Record. 1022*, Transportation Research Board, Washington, D.C., 52–59.
Witczak, M. W., and Uzan, J. (1988). "The universal airport pavement design system rep. I. Granular material characterization." *Rep. Prepared for Dept. of Civil Engineering*, Univ. of Maryland at College Park, College Park, Md.
Zaghloul, S. M., and White, T. D. (1993). "Use of a three-dimensional, dynamic finite element program for analysis of flexible pavement." *Transportation Research Record. 1388*, Transportation Research Board, Washington, D.C., 60–69.

Int. J. Geomech., 2009, 9(5): 195-208